Observations of a Two-Stage Solar Eruptive Event (SEE): Evidence for Secondary Heating

Yang Su[1,2,3]

yang.su@uni-graz.at

Brian R. Dennis[1]

Gordon D. Holman[1]

Tongjiang Wang[1,2]

Phillip C. Chamberlin[1]

Sabrina Savage[1]

Astrid Veronig[3]

Updated January 5, 2012

ABSTRACT

We present RHESSI, SDO/AIA, SOHO/LASCO, STEREO, and GOES observations of a partially occulted solar eruptive event (SEE) that occurred at the South-West limb on 8 March, 2011. The GOES X-ray light curve shows two peaks separated by almost two hours that we interpret as two stages of a single

[1]Solar Physics Laboratory (Code 671), Heliophysics Science Division, NASA Goddard Space Flight Center, Greenbelt, MD 20771, USA

[2]Department of Physics, The Catholic University of America, Washington, DC 20064, USA

[3]Institute of Physics, University of Graz, Universitaetsplatz 5, Graz, 8010, Austria

event associated with the delayed eruption of a CME. A hot flux rope formed during the first stage and continued expanding and rising throughout the event. The speed of the flux rope decreased from ∼120 to 14 km s^{-1} during the decay phase of the first stage and increased again during the second stage to become the CME with a speed of ∼516 km s^{-1}. RHESSI and GOES data analyses show that the plasma temperature reached over 20 MK in the first stage, then decreased to ∼10 MK and increased to 15 MK in the second stage. This event provides clear evidence for a secondary heating phase.

The enhanced EUV and X-ray emission came from the high corona (∼60 arcsec above the limb) in the second stage, ∼40 arcsec higher than the site of the initial flare emission. STEREO-A on-disk observations indicate that the post-flare loops during this stage were of larger scale sizes and spatially distinct from those in the first stage.

Subject headings: Sun: flares – Sun: coronal mass ejections (CMEs) – Sun: X-rays, gamma rays – Sun: UV radiation

1. INTRODUCTION

In the standard model of an impulsive solar flare (see, for example, Shibata et al. 1995; Shibata 1998; Tsuneta 1997), energy is released from the coronal magnetic field by a reconnection process. As a result, plasma is heated to $\gtrsim$10 MK and particles - electrons and ions - are accelerated to relativistic energies. When the flare is accompanied by an eruption, i.e., a jet or a CME, the event is known as a Solar Eruptive Event (SEE). These are the most geoeffective events, since they can subsequently affect the Earth's space environment.

Based on observations from the full-Sun EUV Variability Experiment (EVE) (Woods

et al. 2010) on the Solar Dynamics Observatory (SDO), Woods et al. (2011) have shown the existence of large secondary peaks in the EUV light curves of some flares that can occur many minutes to hours after the initial impulsive energy release that, in other respects, appear to be consistent with the standard flare model. They have argued that, in some cases, these secondary peaks represent additional episodes of energy release in the corona that heat plasma to temperatures of a few MK. Not only are the secondary peaks delayed in time from the impulsive emission, but they have larger scale sizes (based on SDO/AIA images in the EUV), indicating a significantly higher altitude than the site of the earlier, more impulsive emission. However, since these reported secondary events are significantly cooler than the initially heated plasma and are not detected in GOES soft X-ray light curves, there is always the possibility that they merely reflect the cooling of the previously heated plasma into the temperature range of the particular EVE passbands that are sensitive to emission from lower temperature plasma.

Indeed, in the 2010-May-5 event for which Woods et al. (2011) conclude that secondary heating is likely, there is evidence that hot plasma was present during the initial energy release at the location of the source of the secondary emission up to an hour later (seen in AIA 94 Å emission, as presented by Hock et al., private communication). It is possible that the hot plasma cooled on time scales commensurate with conductive and radiative cooling times, as was the case in Aschwanden et al. (2009), who reported on post-flare EUV emission detected with STEREO/EUVI. They attribute the later EUV emission to the cooling of the soft-X-ray-emitting flare loops until they emit radiation detectable in the four spectral passbands covered by that instrument. In one well-observed event seen with both STEREO-A and -B, they were able to estimate a ∼40-min conductive and radiative cooling time of the stereoscopically imaged loops that they argued was consistent with the observed delay of one hour between the initial and secondary peaks in the soft X-ray and EUV light curves.

None of the events studied in Woods et al. (2011) had an increase in the GOES X-ray flux during the late phase. Can plasma be heated to a higher temperature than a few MK during the secondary heating phase (Woods et al. 2011) so that it can be detected in X-rays? In that case, a temperature diagnostic which can show the increase of plasma temperature in the second peak is critical evidence for a secondary heating phase.

In this letter, we present SDO/AIA, STEREO, RHESSI, and GOES observations for a solar eruptive event that showed two GOES peaks separated by about 110 minutes and an associated two-stage CME eruption. This long time delay and increased plasma temperature (from 10 MK to 15 MK) at the time of the secondary peak demonstrate that the second peak could not be the result of the cooling of the plasma heated during the first peak, but was rather from a second episode of energy release. Additional evidence for this scenario comes from observations that show the EUV emission imaged with AIA, and the X-ray emission imaged with RHESSI during the second stage, all come from about 40 arcsec above the site of the initial flare emission.

2. Event Overview

The event reported here occurred on 2011 March 8 on the south-west limb as seen from the Earth. It was well observed by a variety of instruments, including RHESSI, SOHO, SDO, GOES, HINODE, and BBSO. STEREO-A observed the event near disk center from a separation angle with Earth of 87 degrees.

The Atmospheric Imaging Assembly (AIA, Lemen et al. 2011) on the Solar Dynamics Observatory (SDO) images the solar atmosphere in ten UV and EUV passbands covering temperatures from ∼5,000 K to ∼20 MK with high spatial resolution (0.6 arcsec) and cadence (12 s). The Reuven Ramaty High Energy Solar Spectroscopic Imager (RHESSI, Lin et al.

2002) observes solar X-ray and gamma ray emission above 3 keV with high cadence (4 s), spatial resolution (∼3 arcsec), and energy resolution (∼1 keV). It provides information on thermal plasma over ∼8 MK and accelerated electrons with energies above ∼10 keV. In addition, STEREO-A (EUVI, Wuelser et al. 2004) observed the EUV emission of the active region from above at 304, 171, 195, and 284 Å wavelength with spatial resolution of 1.6 arcsec and cadence from 75 s to 5 minutes. These four passbands observe mostly the plasma at temperature from ∼0.1 to ∼2 MK, although the 195 Å channel has a secondary peak in sensitivity at log T(K) = 7.2.

Both the RHESSI and GOES X-ray light curves (see Figure 1a) show two peaks separated by almost two hours (∼108 minutes) that are identified as two individual M-class flares. The first peak (M4.4) started with an impulsive rise in the GOES 1-8 Å channel starting at 18:08 UT and peaking at 18:28 UT. The second, more gradual rise started at 19:46 UT, or even earlier if the decay of the X-ray flux from the first peak is subtracted, and peaked at the M1.4 level at 20:16 UT. The decay to background took about four hours. The small peak at ∼19:00 UT was from a different active region close to the disk center.

Seven AIA EUV light curves integrated over the entire flare region covering 400×500 arcsec^2 are shown in Fig.1(b). The AIA 131 Å passband (with a peak sensitivity at ∼0.5 MK and a secondary peak at ∼11 MK) best agrees with the GOES light curve (as pointed out by Cheng et al. 2011; Woods et al. 2011). Figs. 1(c) and 1(d) show the AIA flux integrated over region A and B in Figure 2, respectively. The light curves of AIA 94, 131 and 193 Å from Region B (higher altitude) all show an increase in their light curves during the first GOES peak, which indicates heating at the same time. The AIA 335 Å (∼3 MK) from Region B had a decrease during the first GOES peak and two gradual increases thereafter, which might be from the cooling of the plasma that produced the two GOES peaks, respectively. This idea is supported by the light curve of AIA 94 Å (∼6 MK) which also shows two gradual

increases after the first GOES peak, but peaks earlier than the AIA 335 Å. This is different from the results of AIA 335 Å for the 2010-May-5 event in Woods et al. (2011), which shows only one peak after the first GOES peak.

Fig.1(e) shows the irradiance change at different temperatures derived from the SDO/EVE data. The plasma temperatures (T) and emission measures (EM) derived independently from the two GOES channels and RHESSI spectra are shown in Fig.1(f). One isothermal component, one thick-target nonthermal component (Thick2 in SSW/OSPEX) and two instrumental lines (when needed) were used to obtain acceptable spectral fits to the RHESSI data. Only the thermal component was needed for spectra in the decay phase around 18:45 UT. The RHESSI temperatures reached over 20 MK in the first peak and 15 MK in the second peak with similar values obtained from the GOES data. The increased irradiance at these high temperatures and at 12.6 and 7.9 MK as derived from EVE data shows that a heating phase must have occurred to produce the second GOES peak.

The two GOES peaks occurred in the same active region and appeared to be associated with the delayed eruption of a CME. Figure 2 shows SDO/AIA images from three channels, 131, 171 ($\sim$0.6 MK) and 211 Å ($\sim$2 MK), at four selected times, two during the first stage and two during the second stage (see the online movie for the entire event). These images show the formation of a hot flux rope during the first stage and the eruption of the same flux rope during the second.

2.1. First Stage, 18:10-19:30 UT, Formation of Flux Rope

The first stage was first observed in all AIA EUV channels when an eruption appeared above the limb at 18:10 UT. RHESSI's 4-6 keV X-ray source was compact and low (about 10 arcsec above the limb) at this time and became extended towards the high corona following

the erupting front (see Figure 3, middle panel, and the online movie). The bright structure (first image at 171 Å in Figure 2) reached a height of ∼55 arcsec above the limb at 18:16 UT. The loops ∼150 arcsec above the limb seen in 171 and 211 Å (1st and 2nd images in Figure 2 at 171 Å) started expanding and rising after the eruption. STEREO-A also observed this expansion but these loops did not erupt as a CME.

The bright erupting feature seen in all AIA EUV channels separated into two parts at 18:15 UT. The upper part continued to rise but disappeared about 1 minute later and the lower part dropped back. A hot flux rope formed underneath the upper part continued to rise at a speed of ∼70 km s^{-1}, accelerate to ∼120 km s^{-1} at the GOES X-ray peak time, and then slowed down to about 14 km s^{-1} after 19:10 UT (see Figure 4). After 18:29 UT, the newly formed hot flux rope is visible in the AIA 131 Å (∼0.5 MK, 11 MK) image but not in AIA 171 (∼ 0.6 MK) Å (see the second image of AIA 131 and 171 Å in Figure 2). The sequence of appearance in different channels, from 131/94/193 to 335, then to 211, then to 193, and then to 171 Å, indicates that the flux rope cooled down from over 10 MK to ∼1 MK as it expanded and rose (see online movie and the color change from blue to green and then to red in the stack plot for AIA 211, 335 and 94 Å in Figure 4).

The hard X-rays above 25 keV had two major peaks during the first stage (Figure 1a), one at 18:13 UT and the other at 18:19 UT. At ∼18:14 UT, the 10-14 keV image shows a loop-top thermal source and an extended structure above it (the first image in Figure 3), while the high energy 30-50 keV image shows a similar elongated nonthermal source in the corona and emission from the flaring loops. At ∼18:19 UT, the time of the second HXR peak, the 10-14 keV source shows a Y-shaped structure high in the corona above the loop-top source, which agrees with the structure seen in AIA 193 Å images.

2.2. Second Stage, 19:30-00:40 UT, Eruption of the Flux Rope

The second stage started with an eruption around 19:33 UT seen in AIA 131Å images after a build up of loops (3rd image at 131 Å in Figure 2). A fine bright line appeared at the start of the second peak (3rd image at 131 Å in Figure 2) followed by an elongated "X"-shaped structure (4th image at 131 Å in Figure 2) with initially turbulence below, and later the appearance of rapidly falling new bright loops (see the online movie). Emission above the X-point was much fainter but suggested that hot plasma was also driven to higher altitudes at the same time.

The flux rope formed during the first stage accelerated again after ∼19:12 UT to about 100 km s^{-1} before it moved out of the AIA field of view. The average acceleration rate was about 0.11 km s^{-2} after 19:30 UT. It reappeared as the CME shown in the SOHO/LASCO image in Figure 4, first seen at 20:12 UT with an average speed of ∼516 km s^{-1}.

Downflows (McKenzie & Hudson 1999; Savage & McKenzie 2011) are clearly seen above the arcade region in AIA 193 Å images during the second stage (4th image at 131Å in Figure 2, and 3rd and 4th image at 131 and 193 Å, respectively, in Figure 3). Plasma at lower altitude under the down flows and above the loops was heated at this time, resulting in an increase in the EUV emission from the higher temperature AIA passbands (131 and 193 Å, see Figure 1 and 3) and in the soft X-ray emission imaged by RHESSI (bottom panel in Figure 3). The RHESSI and GOES data show that the temperature peaked at ∼15 MK.

We do see a later peak in the AIA cooler channels (171, 211, 193, 304 and 335 Å) around 20:52 UT (Figure 1b). The fact that the flux in the 94 and 131 Å passbands peaked earlier than the fluxes in those cooler channels suggests that this peak in the cooler channels is from the cooling of the plasma heated in the second stage, although an additional heating episode in the same active region is not ruled out.

3. Discussion

The eruptive event on 2011 March 8 had two stages, the first with impulsive X-ray emission and the second with more gradual emission. A hot flux rope (over 10 MK) formed in the first stage and rose with a speed of up to 120 km s^{-1} at ∼18:30 UT. It cooled and slowed down to about 14 km s^{-1} but kept rising and expanding during the decay of the first GOES peak. The same flux rope accelerated again and erupted during the second stage, presumably to appear later as the CME seen with LASCO. At the same time, plasma was heated to about 15 MK at a location above the initial loop arcade formed during the first stage. STEREO-A observations (Figure 5) also show that the scale sizes of the flare loops in the second stage were larger than that of the loop arcade in the first stage. This is consistent with the findings of Woods et al. (2011) for the 2010-May-5 event. This two-stage eruptive event provides clear evidence for the secondary heating phase.

The differences between our results and those in Woods et al. (2011) are that not only the cooler EUV channels, but also the hotter EUV channels, GOES and RHESSI responded to the second-stage energy release (Figure 1), and that the light curves of AIA 335 Å passband from the higher altitude (Region B) shows two, rather than one, gradual peaks after the first GOES peak. We interpret these two gradual increases as results of the cooling of plasma that were heated to higher temperatures during the two stages. However, since the flux rope passed through the two regions (A and B), it may also contribute in the two light curves.

The base-difference image in the STEREO 171 Å passband in Figure 5 shows a brighting at 18:03 UT, even before the start of the first peak. This observation suggests that the event started behind the limb and therefore gave a rapid rise in the GOES soft X-ray flux and temperature as the initial eruption emerged from behind the limb. In the first stage, RHESSI showed a 30 to 40-arcsec-long X-ray source at both thermal and nonthermal energies extending up into the corona. AIA images in 131 and 193 Å show a similar structure. The

RHESSI thermal sources show a Y-shaped coronal structure at 18:19 UT, similar to that seen in AIA 131 and 193Å.

There are still many unanswered questions related to this event. Is the secondary heating always related to a delayed CME eruption? What is the reason for the decrease in velocity of the flux rope in the fist stage? We will study this event in more detail and search for other similar events to answer these questions.

We thank the referee for providing valuable comments and help in improving this paper. We acknowledge the critical support provided by Kim Tolbert and Richard Schwartz and their help with the IDL RHESSI data analysis software and the SSW procedures. We are grateful to Frederick C. Bruhweiler for managing the NASA Grant NNG06GB96A at The Catholic University of America, through which one of us (YS) was funded. This work is also supported in part by the European Community Framework Programme 7, "High Energy Solar Physics Data in Europe (HESPE)", grant agreement NO.: 263086. The work of T.W. was supported by NASA grants NNX08AE44G and NNX10AN10G.

REFERENCES

Aschwanden, M. J., Wuelser, J. P., Nitta, N. V., & Lemen, J. R. 2009, Sol. Phys., 256, 3

Cheng, X., Zhang, J., Liu, Y., & Ding, M. D. 2011, ApJ, 732, L25

Lemen, J. R., Title, A. M., Akin, D. J., Boerner, P. F., Chou, C., Drake, J. F., Duncan, D. W., Edwards, C. G., Friedlaender, F. M., Heyman, G. F., Hurlburt, N. E., Katz, N. L., Kushner, G. D., Levay, M., Lindgren, R. W., Mathur, D. P., McFeaters, E. L., Mitchell, S., Rehse, R. A., Schrijver, C. J., Springer, L. A., Stern, R. A., Tarbell, T. D., Wuelser, J.-P., Wolfson, C. J., Yanari, C., Bookbinder, J. A., Cheimets, P. N.,

Caldwell, D., Deluca, E. E., Gates, R., Golub, L., Park, S., Podgorski, W. A., Bush, R. I., Scherrer, P. H., Gummin, M. A., Smith, P., Auker, G., Jerram, P., Pool, P., Soufli, R., Windt, D. L., Beardsley, S., Clapp, M., Lang, J., & Waltham, N. 2011, Sol. Phys., 115

Lin, R. P., Dennis, B. R., Hurford, G. J., Smith, D. M., Zehnder, A., Harvey, P. R., Curtis, D. W., Pankow, D., Turin, P., Bester, M., Csillaghy, A., Lewis, M., Madden, N., van Beek, H. F., Appleby, M., Raudorf, T., McTiernan, J., Ramaty, R., Schmahl, E., Schwartz, R., Krucker, S., Abiad, R., Quinn, T., Berg, P., Hashii, M., Sterling, R., Jackson, R., Pratt, R., Campbell, R. D., Malone, D., Landis, D., Barrington-Leigh, C. P., Slassi-Sennou, S., Cork, C., Clark, D., Amato, D., Orwig, L., Boyle, R., Banks, I. S., Shirey, K., Tolbert, A. K., Zarro, D., Snow, F., Thomsen, K., Henneck, R., McHedlishvili, A., Ming, P., Fivian, M., Jordan, J., Wanner, R., Crubb, J., Preble, J., Matranga, M., Benz, A., Hudson, H., Canfield, R. C., Holman, G. D., Crannell, C., Kosugi, T., Emslie, A. G., Vilmer, N., Brown, J. C., Johns-Krull, C., Aschwanden, M., Metcalf, T., & Conway, A. 2002, Sol. Phys., 210, 3

McKenzie, D. E., & Hudson, H. S. 1999, ApJ, 519, L93

Savage, S. L., & McKenzie, D. E. 2011, ApJ, 730, 98

Shibata, K. 1998, in Astrophysics and Space Science Library, Vol. 229, Observational Plasma Astrophysics : Five Years of YOHKOH and Beyond, ed. T. Watanabe & T. Kosugi, 187

Shibata, K., Masuda, S., Shimojo, M., Hara, H., Yokoyama, T., Tsuneta, S., Kosugi, T., & Ogawara, Y. 1995, ApJ, 451, L83

Tsuneta, S. 1997, ApJ, 483, 507

Woods, T. N., Eparvier, F. G., Hock, R., Jones, A. R., Woodraska, D., Judge, D., Didkovsky, L., Lean, J., Mariska, J., Warren, H., McMullin, D., Chamberlin, P., Berthiaume, G., Bailey, S., Fuller-Rowell, T., Sojka, J., Tobiska, W. K., & Viereck, R. 2010, Sol. Phys., 3

Woods, T. N., Hock, R., Eparvier, F., Jones, A. R., Chamberlin, P. C., Klimchuk, J. A., Didkovsky, L., Judge, D., Mariska, J., Warren, H., Schrijver, C. J., Webb, D. F., Bailey, S., & Tobiska, W. K. 2011, ApJ, 739, 59

Wuelser, J.-P., Lemen, J. R., Tarbell, T. D., Wolfson, C. J., Cannon, J. C., Carpenter, B. A., Duncan, D. W., Gradwohl, G. S., Meyer, S. B., Moore, A. S., Navarro, R. L., Pearson, J. D., Rossi, G. R., Springer, L. A., Howard, R. A., Moses, J. D., Newmark, J. S., Delaboudiniere, J.-P., Artzner, G. E., Auchere, F., Bougnet, M., Bouyries, P., Bridou, F., Clotaire, J.-Y., Colas, G., Delmotte, F., Jerome, A., Lamare, M., Mercier, R., Mullot, M., Ravet, M.-F., Song, X., Bothmer, V., & Deutsch, W. 2004, in Society of Photo-Optical Instrumentation Engineers (SPIE) Conference Series, Vol. 5171, Society of Photo-Optical Instrumentation Engineers (SPIE) Conference Series, ed. S. Fineschi & M. A. Gummin, 111–122

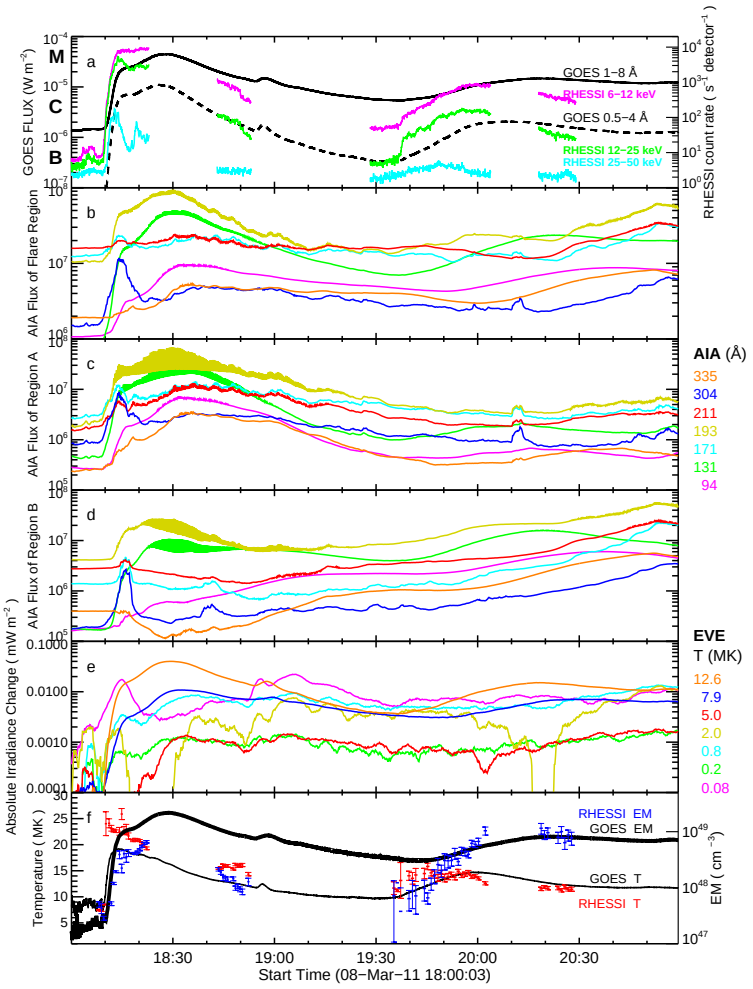

Fig. 1.— Light curves of the 8 March 2011 event: (a) GOES 1-8 Å (black solid line), 0.5-4 Å (black dashed line), RHESSI quick-look count rates from the front segments of detectors 1,3,4,5,7 and 8 at 6-12 keV (red), 12-25 keV (green, divided by 2 for clarity) and 25-50 keV (cyan, divided by 10). The peak at ∼18:56 UT was from a different active region close to disk center. (b) SDO/AIA flux in seven channels integrated over the entire flare region covering 400×500 arcsec^2. Each curve has a different constant flux subtracted for clarity. (c,d) AIA flux integrated over Region A and B shown in Figure 2, respectively. (e) The irradiance change at different temperatures derived from the SDO/EVE data. (f) Time evolution of plasma temperature (T) and emission measure (EM) derived from GOES and RHESSI data. The integration time for RHESSI spectra was 40s before 19:30 UT and 60s after. See the color version in the electronic edition of *The Astrophysical Journal Letters*.

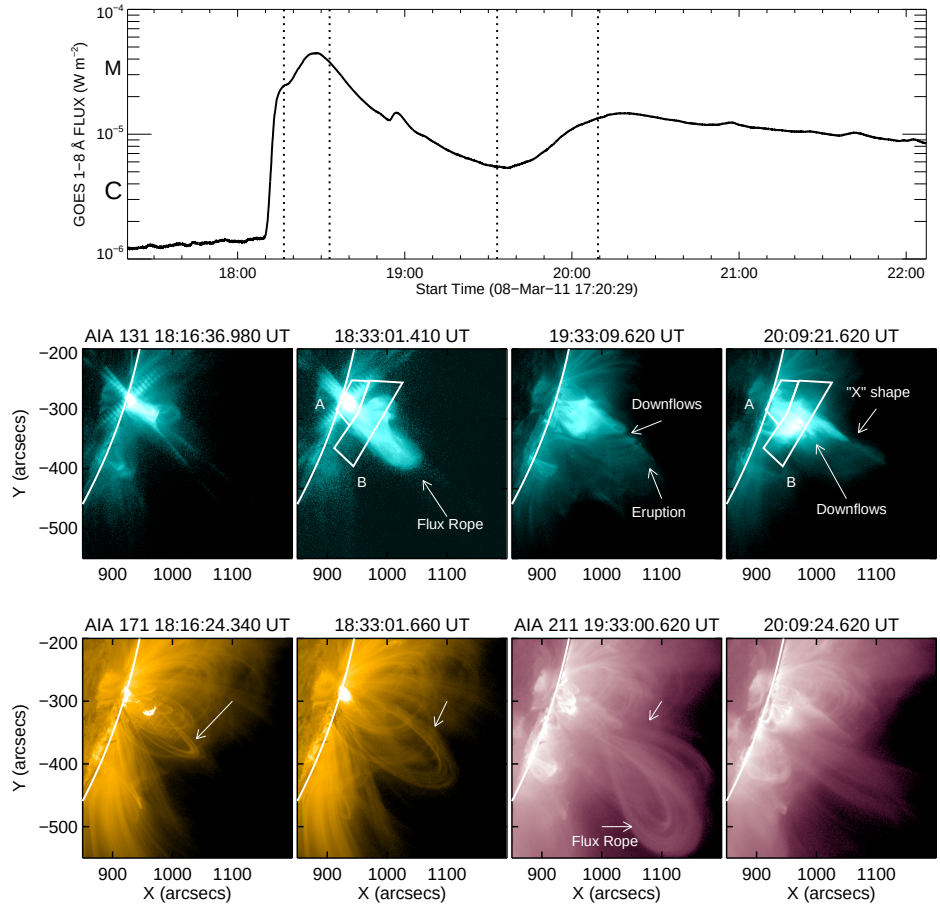

Fig. 2.— Top panel: GOES 1-8 Å light curve with dotted lines showing the times of the images below. The two white boxes marked as A and B show the two regions used to obtain the light curves in Fig. 1, c and d. Middle panel: AIA images in the 131 Å passband. Bottom panel: Images in the 171 and 211 Å passband with the three unlabeled arrows showing the location of expanding loops.

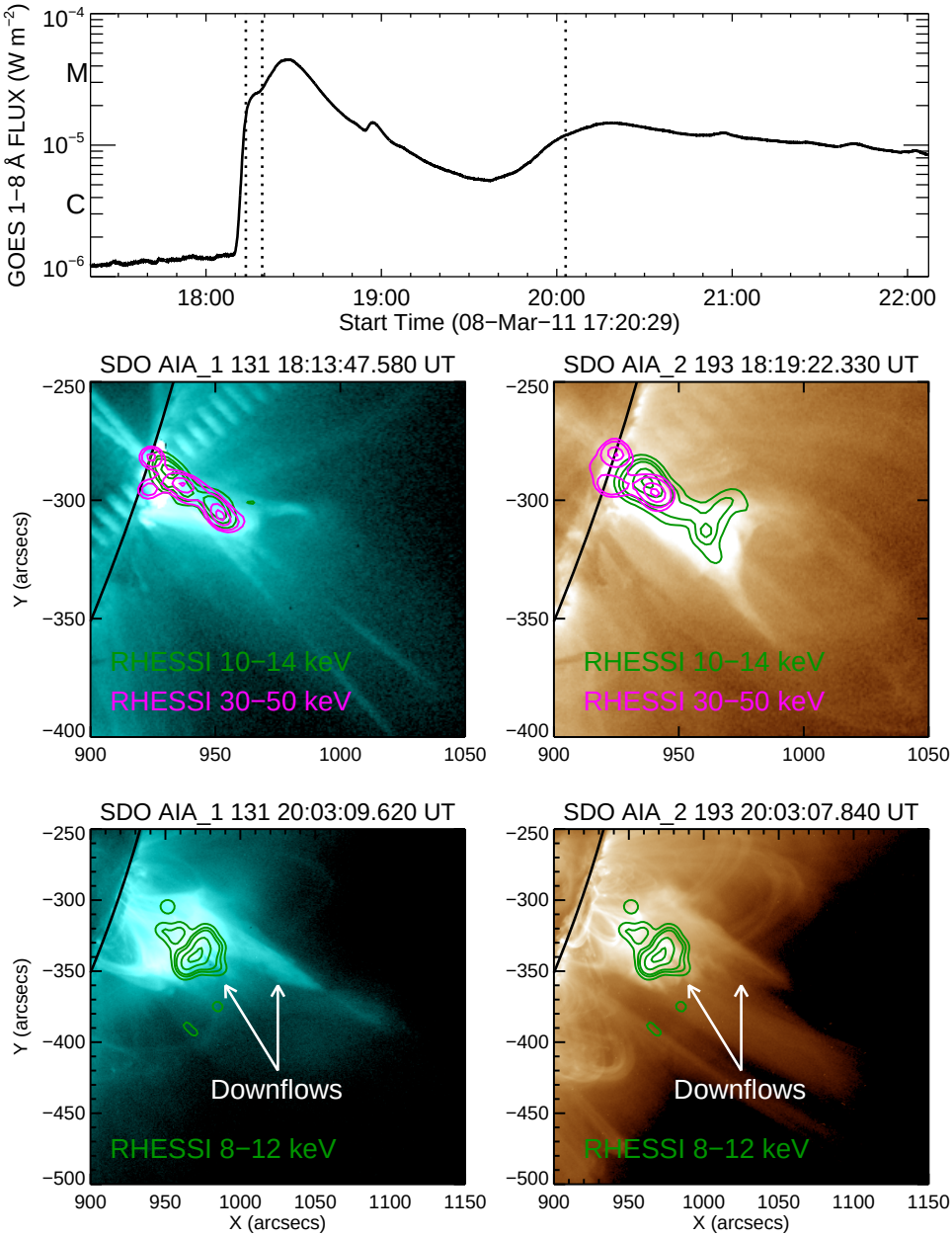

Fig. 3.— Top panel: same as Figure 2 but with different selected times. Middle and bottom panel: AIA 131 and 193 Å images and RHESSI thermal and nonthermal sources at three selected times. The RHESSI images were made using the Pixon and Clean algorithm with detector 3, 4, 5, 8, and 9.

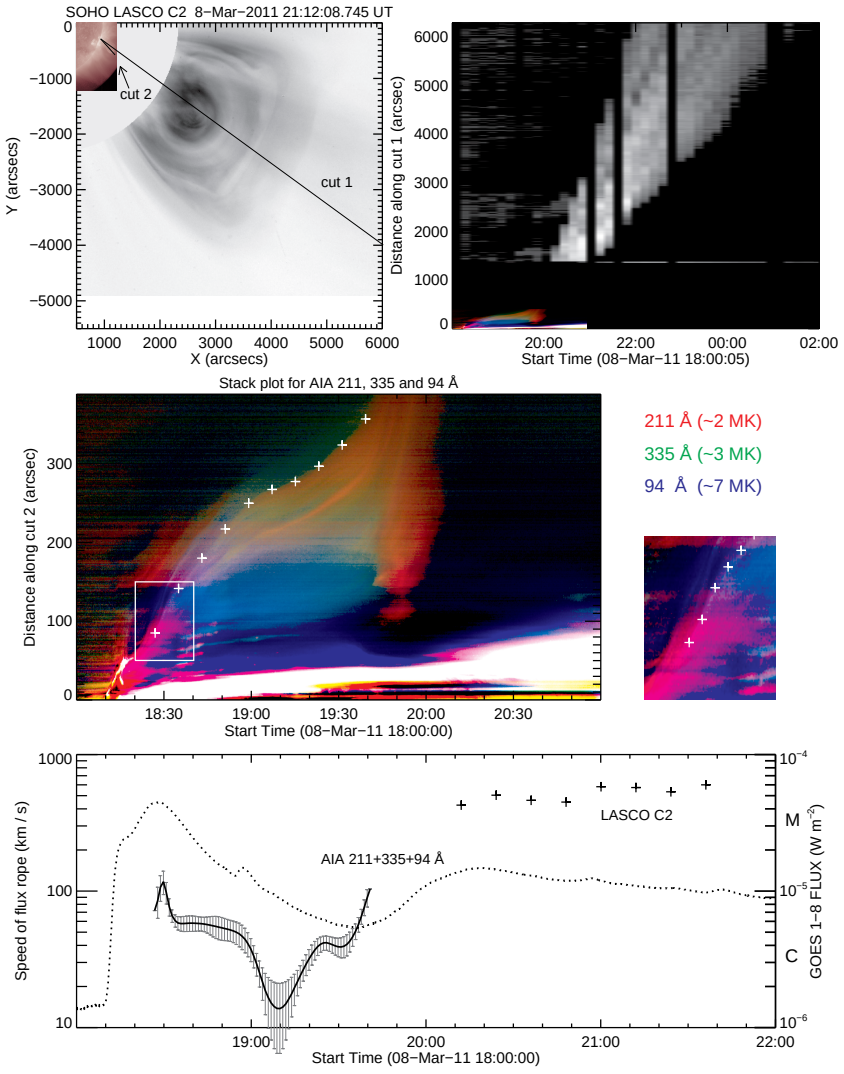

Fig. 4.— Flux rope and CME motion derived from SDO/AIA and SOHO/LASCO data. Top left panel: AIA 211 Å image and the CME observed by LASCO-C2 are shown on the left. The two "cuts" used for the stack plots are indicated by the two black lines. The stack plot in the top right panel shows the time evolution of flux along "cut 1". The black vertical lines are data gaps. Middle panel: Stack plot of "cut 2" for AIA 211 (red), 335 (green), and 94 Å (blue). The image on the right shows the region marked in the left image. The crosses show the edge used to determine the speed of the flux rope. All the stack plots are from base difference images with the reference image at 18:00 UT. Bottom panel: Speed of flux rope as a function of time with GOES 1-8 Å light curve. The ±1 sigma errors on the speed are obtained from 10 independent measurements of the edge of the flux rope based on 1-minute cadence data.

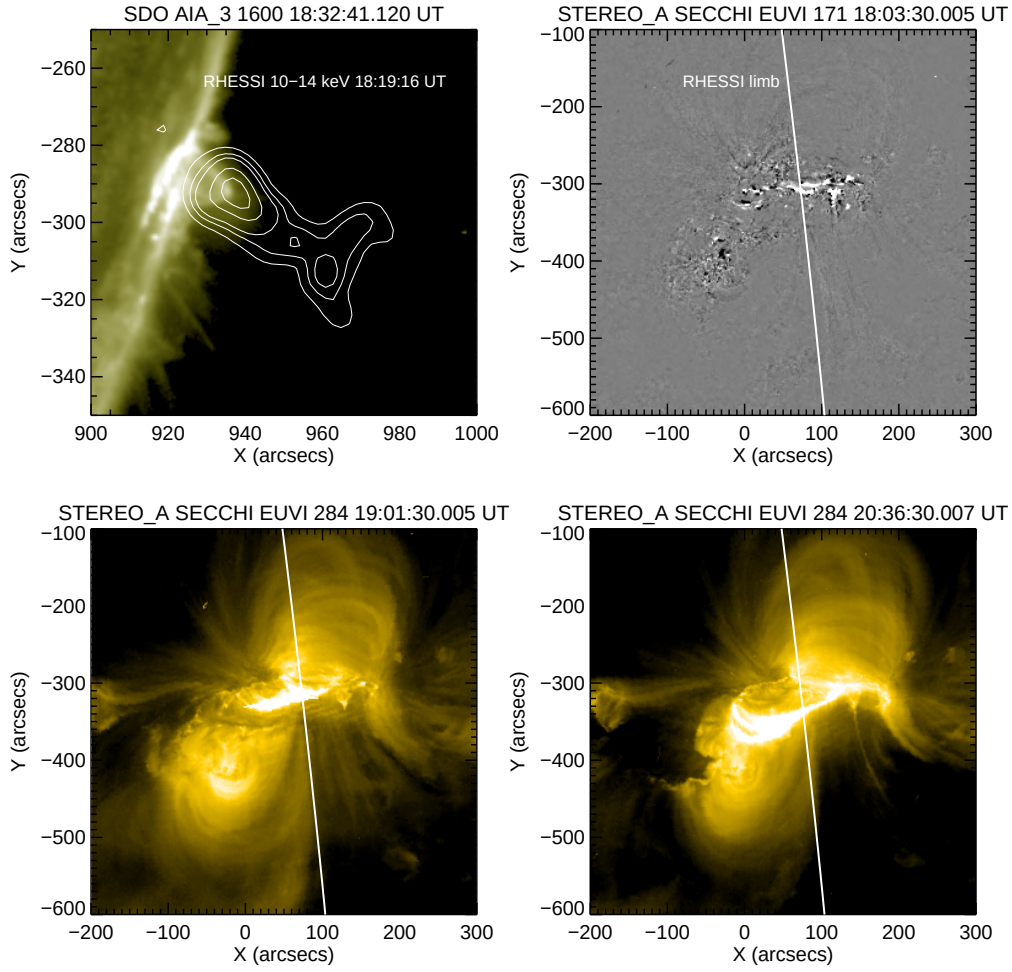

Fig. 5.— Top panel, left: AIA 1600 Å image (18:32 UT) showing parts of the two flare ribbons and flaring loops with RHESSI's 10-14 keV contours (10, 20, 30, 60 and 90% of peak flux) at 18:19:16 UT. Top panel, right: STEREO-A 171 Å passband base difference image showing activity at 18:03:30 UT. The white lines in this image and the two below show the limb as seen from SDO and RHESSI in Earth orbit with the visible disk to the left. Bottom panel: STEREO-A 284 Å observations of post flare loops during the two stages of the event.